

Preparation of $\text{La}_{0.5}\text{Li}_{0.5}\text{TiO}_3$ perovskite thin films by the sol–gel method

K. KITAOKA

Itami Plant, Minolta Co. Ltd, 4-18, Takadai, Itami, Hyogo-Ken 664, Japan

H. KOZUKA, T. HASHIMOTO, T. YOKO

Institute for Chemical Research, Kyoto University, Uji, Kyoto-Fu 611, Japan

Perovskite $\text{La}_{0.5}\text{Li}_{0.5}\text{TiO}_3$ (LLT) thin films, 0.2–1 μm thick, were deposited on non-alkali aluminoborosilicate glass substrates (NA substrates) and glass substrates with ITO (indium tin oxide) coatings (ITO substrates) by the sol–gel method. Alkoxide-based solutions containing titanium alkoxide, lithium alkoxide and lanthanum alkoxide and acetate-based solutions containing titanium alkoxide, lithium acetate and lanthanum acetate, were used as coating solutions. Impurity phases tended to be precipitated on heat treatment in the films derived from the acetate-based solutions. Addition of acetylacetone or partial substitution of lead for lithium in the acetate-based solutions, however, was effective in suppressing the precipitation of impurity phases. Preferred orientation of the LLT (1 1 1/2) plane was observed in the films prepared from the acetate-based solutions when NA substrates were used, whereas the employment of the alkoxide-based solutions or ITO substrates and the partial substitution of lead for lithium, reduced the preferred orientation. The electrical conductivity of the films was much lower than the values reported for the sintered materials.

1. Introduction

All-solid-state electrochromic devices and batteries require solid-state ionic conductors as the electrolyte. Among the solid-state ionic conductors, lithium ion conductors have long been one of the most important target materials for much research [1]. For instance, lithium nitride [2] lithium sulphide and iodide-based glasses [3, 4], and lithium halide compounds [5] are known to have high lithium conductivity at room temperature. Because these non-oxide materials all have less stability against humidity in the ambient atmosphere, development of highly conductive, stable oxide lithium ion conductors is a very important issue. In addition, thin-film conductors are required for applying these materials in electrochromic displays and compact batteries.

Kuwano and West [6] reported that LISICON- γ_{II} type $\text{Li}_{3.5}\text{V}_{0.5}\text{Ge}_{0.5}\text{O}_4$ has an ionic conductivity of $5 \times 10^{-5} \text{ S cm}^{-1}$ in grains at room temperature. Aono *et al.* [7] found that polycrystalline NASICON type $\text{Li}_{1.3}\text{M}_{0.3}\text{Ti}_{1.7}(\text{PO}_4)_3$ ($\text{M} = \text{Al}$ and Sc) exhibits high ionic conductivities of $3 \times 10^{-3} \text{ S cm}^{-1}$ in grains and $7 \times 10^{-4} \text{ S cm}^{-1}$ in the bulk at room temperature. Recently, Inaguma *et al.* [8] prepared lithium-deficient perovskite $\text{La}_{0.5}\text{Li}_{0.5-x}\text{TiO}_{3-y}$, reporting ionic conductivities of $10^{-3} \text{ S cm}^{-1}$ in grains and $2 \times 10^{-5} \text{ S cm}^{-1}$ in the bulk at room temperature, which are as high as those of $\text{Li}_{1.3}\text{M}_{0.3}\text{Ti}_{1.7}(\text{PO}_4)_3$. As far as $\text{La}_{0.5}\text{Li}_{0.5}\text{TiO}_3$ (LLT) is concerned, Brous *et al.* [9] and Patil and Chincholkar [10] showed that LLT has the cubic structure, and Varaprasad *et al.*

[11] reported that LLT has the tetragonal, tungsten bronze structure with the coexistence of ferroelectric and antiferroelectric domains and has a high dielectric constant peak value of 37000. Kochergina *et al.* [12] also reported that LLT is of tetragonal tungsten bronze structure and exhibits semiconducting behaviour. The crystal structure, ionic deficiency, and electrical properties of LLT are thus influenced by the preparation conditions, and LLT is an interesting material as a new lithium ion conductor.

So far, LLT has been prepared from powder mixtures of oxides and carbonates by solid-state reaction, but no attempts have been made to prepare it in a form of thin film, which is important for applying these materials in devices. In the present study, we prepared LLT thin films by the sol–gel method to study the effects of the compositions of the starting solutions and the substrate material on the crystalline phases, the orientation of the crystals, and the microstructure of the films. The electrical conductivity of the films was also measured.

2. Experimental procedure

2.1. Preparation of the starting solutions

Three series of solutions, listed in Tables I–III were prepared. In all cases, titaniumisopropoxide was used as the titanium source. Series 1 solutions are alkoxide-based, series 2 solutions are acetate-based, and series 3 solutions are acetate-based and lead-containing solutions. The procedures for preparing series 1, 2 and 3 solutions are illustrated in Fig. 1a–c, respectively.

TABLE I Composition of series 1 solutions

Solution	Mole ratio					
	La(OPr ⁱ) ₃	Li	Ti(OPr ⁱ) ₄	CH ₃ OCH ₂ CH ₂ OH	H ₂ O	HNO ₃
1-a	0.5	0.5	1.0	35.0	2.58	0.25
1-b	0.5	0.5	1.0	35.0	2.0	
1-c	0.5	0.5	1.0	45.0		

TABLE II Composition of series 2 solutions

Solution	Mole ratio						
	La(CH ₃ COO) ₃ ·1.5H ₂ O	LiCH ₃ COO·2H ₂ O	Ti(OPr ⁱ) ₄	CH ₃ OCH ₂ CH ₂ OH	CH ₃ COCH ₂ COCH ₃	HCl	H ₂ O
2-a	0.5	0.5	1.0	30.0		1.0	18.25
2-b	0.5	0.5	1.0	30.0		1.0	8.25
2-c	0.5	0.5	1.0	30.0		1.0	3.76
2-d	0.5	0.5	1.0	30.0	0.5	1.0	3.76

TABLE III Composition of series 3 solutions

Solution	Mole ratio						
	La(CH ₃ COO) ₃ ·1.5H ₂ O	LiCH ₃ COO·2H ₂ O	Pb(CH ₃ COO) ₂ ·3H ₂ O	Ti(OPr ⁱ) ₄	CH ₃ OCH ₂ CH ₂ OH	HNO ₃	H ₂ O
3-a	0.5	0.5	0.05	1.0	30.0	1.2	2.8
3-b	0.5	0.4	0.10	1.0	30.0	1.2	2.8
3-c	0.5	0.3	0.15	1.0	30.0	1.2	2.8
3-d	0.5	0.2	0.20	1.0	30.0	1.2	2.8
3-e	0.5	0.1	0.25	1.0	30.0	1.2	2.8

2.1.1. Series 1 solutions (Fig. 1a)

First, lithium 2-methoxyethoxide solution was prepared by dissolving lithium metal (Nacalai Tesque) in 2-methoxyethanol (Nacalai Tesque) in flowing dry nitrogen. After adding lanthanum isopropoxide (Kojundokagaku Laboratory) and titanium isopropoxide (Wako Pure Chemical Industries), the solution was refluxed at 105 °C for 1 h, and the solution of 2-methoxyethanol, ion-exchanged water and concentrated nitric acid (Nacalai Tesque) was added.

2.1.2. Series 2 solutions (Fig. 1b)

Lanthanum acetate 1.5 hydrate (Nacalai Tesque), lithium acetate dihydrate (Nacalai Tesque) and ion-exchanged water were dissolved successively in the solution of 2-methoxyethanol, concentrated hydrochloric acid (Nacalai Tesque) and ion-exchanged water. Then the solution of titanium isopropoxide, 2-methoxyethanol and acetylacetone was added.

2.1.3. Series 3 solutions (Fig. 1c)

Lanthanum acetate 1.5 hydrate, lithium acetate dihydrate and lead acetate trihydrate (Nacalai Tesque) were dissolved successively in the solution of 2-methoxyethanol, concentrated nitric acid and ion-exchanged water. Then the solution of titanium isopropoxide and 2-methoxyethanol was added.

2.2. Preparation of the samples

Aluminoborosilicate non-alkali glass plates (NA substrate) and non-alkali glass plates with ITO coatings (ITO substrate) were used as the substrate materials. Dip coating was performed using the above solutions at room temperature with a withdrawing rate of 45 mm min⁻¹. Dip coating and heat treatment were repeated to obtain thin film samples.

The above solutions were concentrated and gelled at 150 °C, and the resultant gels were dried at 200 °C. The dried gel pieces were heated at 600–1300 °C for 2 h to obtain powder samples.

2.3. Measurements

Compositions of the thin-film samples were determined with an inductively coupled plasma arc emission spectrometer (ICP; Shimadzu Manufacturing, GEW-170P ICPS-2H) and an atomic absorption analyser (Nihon Jarelash, AA-1). The thin film samples were dissolved in hot hydrochloric acid containing a small quantity of hydrogen peroxide. The lanthanum and titanium contents in the solution were measured with ICP, and the lithium contents were measured with atomic absorption analysis.

Crystalline phases were analysed for the film and powder samples using an X-ray diffractometer (Rigaku, RAD IIA) with CuK_α radiation. The crystallite size was determined using Scherrer's equation. The

thickness of the thin film samples was measured with a surface profilometer (Kosaka Laboratory, SE30D) and by observing the fracture surface with a scanning electron microscope (SEM) (Hitachi Manufacturing Co., 450S). Refractive indices of the thin film samples were measured with an ellipsometer (Mizojiri Kogaku, DVA-36VW) with a light of 633 nm. The microstructure of the thin film surface was observed with SEM.

In-plane a.c. electrical conductivity of the film was measured by impedance analysis using a frequency response analyser (NF Electric Instruments, 5090). The thin film samples deposited on NA substrates were used for the measurements. Gold electrodes were deposited on the surface of the thin film samples, and

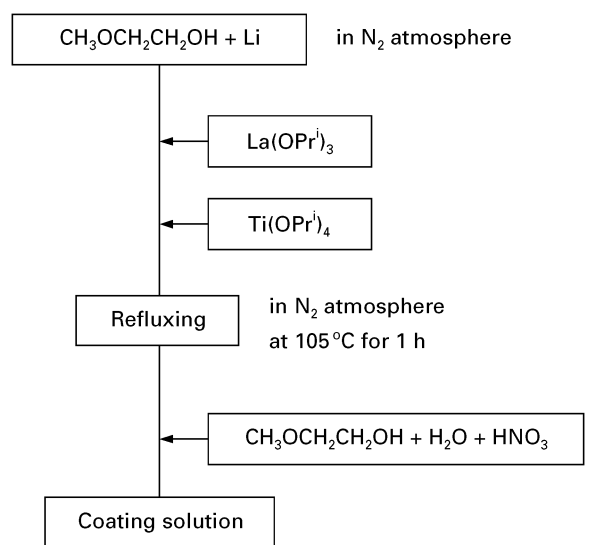
the measurements were performed in an argon gas atmosphere.

3. Results

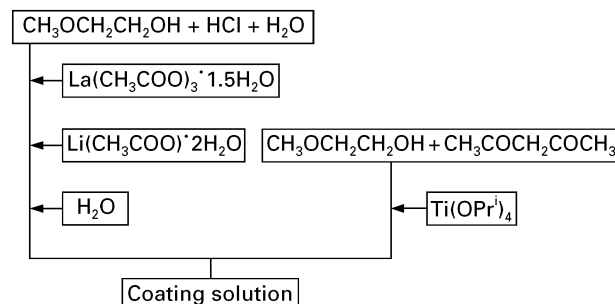
3.1. Compositions of the thin film samples
Table IV shows the analysed compositions of the thin film samples deposited on ITO substrates. The analysed compositions were $\text{La}_{0.52}\text{Li}_{0.42}\text{TiO}_{2.99}$ and $\text{La}_{0.53}\text{Li}_{0.21}\text{TiO}_{2.90}$ for the film samples prepared from solutions 1-b and 2-b, respectively, indicating the reduction of lithium content on heat treatment. The lithium content was much less for the film from 2b than from 1b. It should be noted that the deficiency of lithium, which is important for high lithium conductivity [8] could be attained at much lower heating temperatures than those prepared via solid-state reaction by Inaguma *et al.* (1300 °C) [8].

3.2. X-ray diffraction

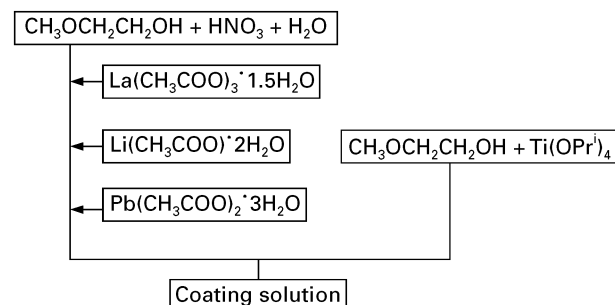
Fig. 2 shows the XRD patterns of the thin film samples prepared from solution 1-b, which is an alkoxide-based series 1 solution. For the film deposited on ITO substrate, besides the diffraction peaks of ITO, perovskite LLT (110), (111) and (111/2) peaks were



(a)



(b)



(c)

Figure 1 Flow charts for preparing the coating solutions of (a) series 1, (b) series 2 and (c) series 3.

TABLE IV Compositions of the thin-film samples deposited on ITO substrates from solutions 1-b and 2-b. Dip-coating and heat treatment at 700 °C were repeated 20 times

Solution	La (at %)	Li (at %)	Ti (at %)	Calculated composition
1-b	26.8	21.5	51.7	$\text{La}_{0.52}\text{Li}_{0.42}\text{TiO}_{2.99}$
2-b	30.2	12.3	57.5	$\text{La}_{0.53}\text{Li}_{0.21}\text{TiO}_{2.90}$

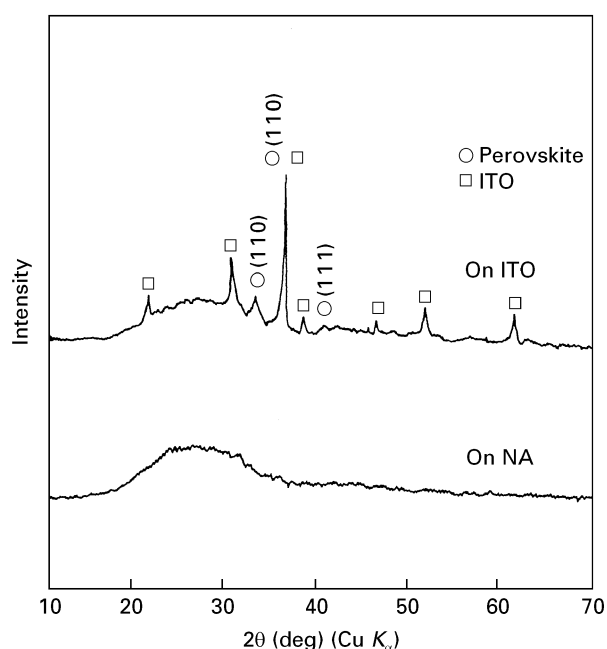


Figure 2 XRD patterns of $\text{La}_{0.5}\text{Li}_{0.5}\text{TiO}_3$ films prepared on ITO and NA substrates from solution 1-b. Dip-coating and heat treatment at 700 °C were repeated five times. The film thickness was about 0.2 μm.

observed, where the LLT (111/2) peak overlaps with the ITO (400) peak. No evident difference was found in the XRD patterns between the films derived from series 1 solutions with or without water or nitric acid. In contrast, for the solution 1-derived films deposited on NA substrate, no diffraction peaks were observed, indicating that the films are amorphous.

Fig. 3 shows the XRD patterns of the thin film samples prepared from series 2 solutions. The patterns of the films deposited on ITO and NA substrates are shown in Fig. 3a and b, respectively. On ITO substrate, LLT (111), (110) and (111/2) peaks were observed as seen in Fig. 3a. As the $\text{H}_2\text{O}/\text{Ti}(\text{OC}_3\text{H}_7)_4$ mole ratio was increased from 5.51 to 20 in the starting solution without the addition of acetylacetonate, the diffraction peaks at $2\theta = 26.4^\circ$, 27.0° and 27.9° , which are attributed to $\text{La}_2\text{Ti}_2\text{O}_7$ crystals, slightly increased in intensity (Fig. 3a, 2-a–2-c). When acetylacetonate was added (solution 2-d), the LLT (110) peak disappeared and the impurity peaks at $2\theta = 26.4^\circ$, 27.0° and 27.9° decreased. In contrast, for the solution 2-derived films deposited on NA substrate, no other peak than LLT (111/2) was observed irrespective of the solution compositions, namely, the amount of water and with or without acetylacetonate.

Fig. 4 shows the XRD patterns of the thin film samples prepared from lead-containing, acetate-based, series 3 solutions. The patterns of the films deposited on ITO and NA substrates are shown in Fig. 4a and b, respectively. For the samples deposited on ITO substrates, LLT (111), (110) and (111/2) peaks were observed with no impurity peaks, irrespective of the lead contents, suggesting the formation of $\text{La}_{0.5}(\text{Li}, \text{Pb})_{0.5}\text{TiO}_3$ perovskite solid solution. It should be noted that the introduction of lead suppresses the precipitation of impurity phases that were observed in the films from series 2 solutions. As the lead content increased, the LLT (100) peak emerged and the (110) peak increased. On the other hand, for the films deposited on NA substrates, the LLT (100), (110) and (200) peaks increased in intensity and the preferred orientation of the LLT (111) plane diminished as the lead content increased.

Fig. 5a and b show the XRD patterns of the powder samples obtained by heat-treating the dried gel pieces prepared from solution 1-b and 2-b, respectively. In the sample from alkoxide-based solution 1-b, LLT was precipitated at 600°C and the LLT diffraction peaks grew with increasing heating temperature. In contrast, in the sample from the acetate-based solution 2-b, $\text{La}_2\text{Ti}_2\text{O}_7$ was precipitated at 600°C and LiTi_2O_4 was additionally precipitated at 700°C without the formation of LLT. Even heat-treatment at higher temperatures did not result in the LLT formation.

As listed in Table V, the crystallite size was 13, 17 and 13 nm for the thin film samples that were prepared from solutions 1-b, 2-b and 3-c, respectively, by repeating dip-coating on ITO substrates and heat-treatment at 700°C for 10 min, 20 times.

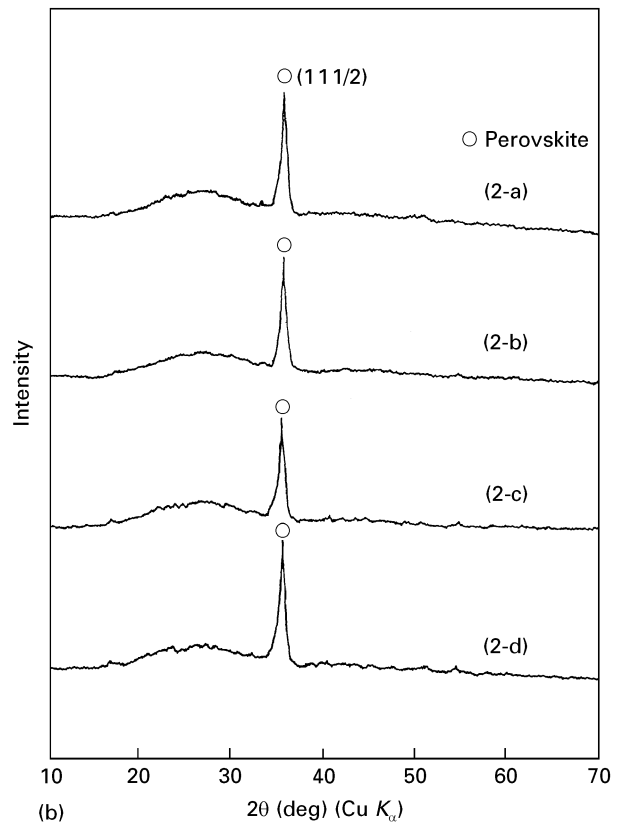
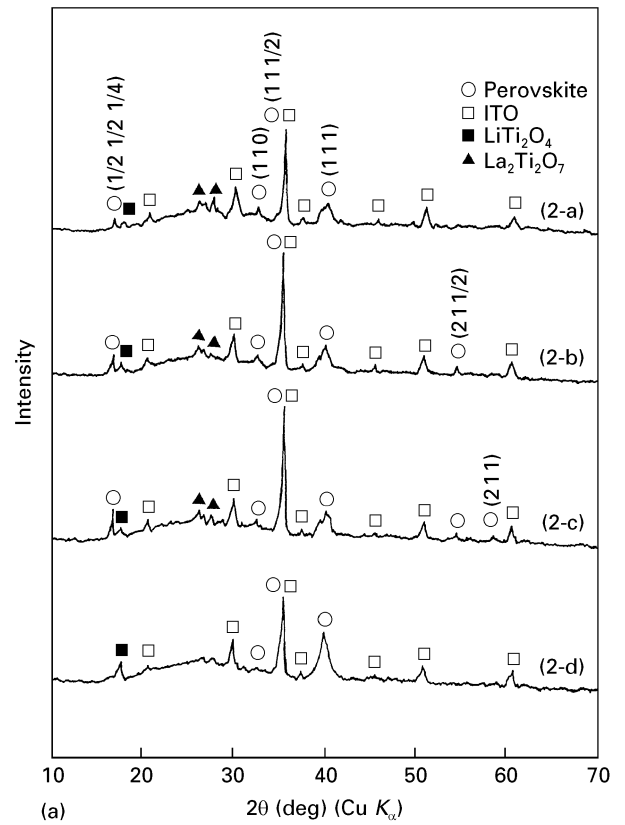
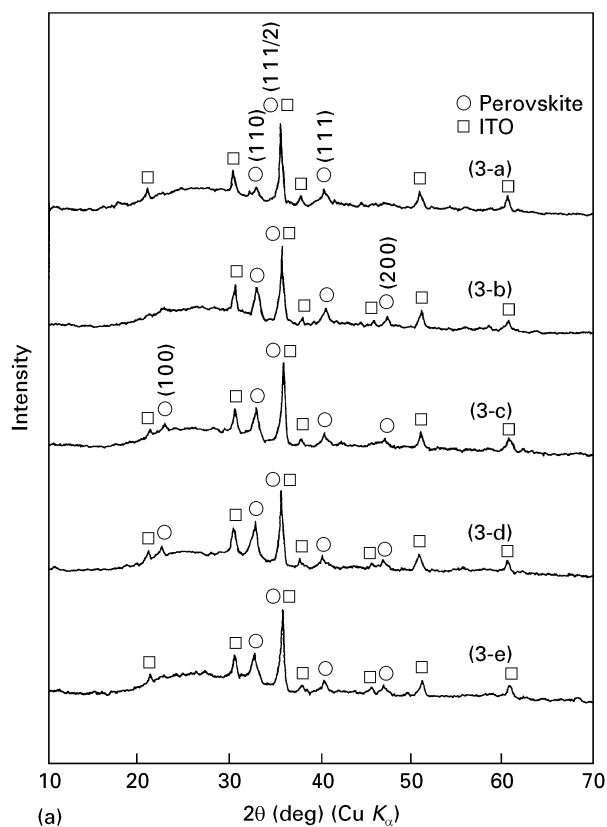


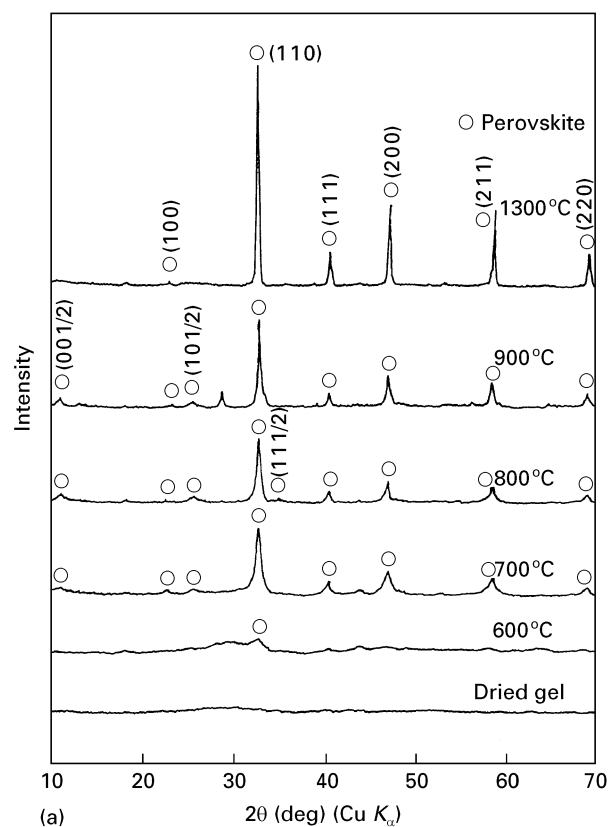
Figure 3 XRD patterns of $\text{La}_{0.5}\text{Li}_{0.5}\text{TiO}_3$ films prepared on (a) ITO and (b) NA substrates from series 2 solutions. Dip-coating and heat treatment at 700°C were repeated 10 times. The film thickness was about $0.45\ \mu\text{m}$.

3.3. Microstructure of the thin film surface

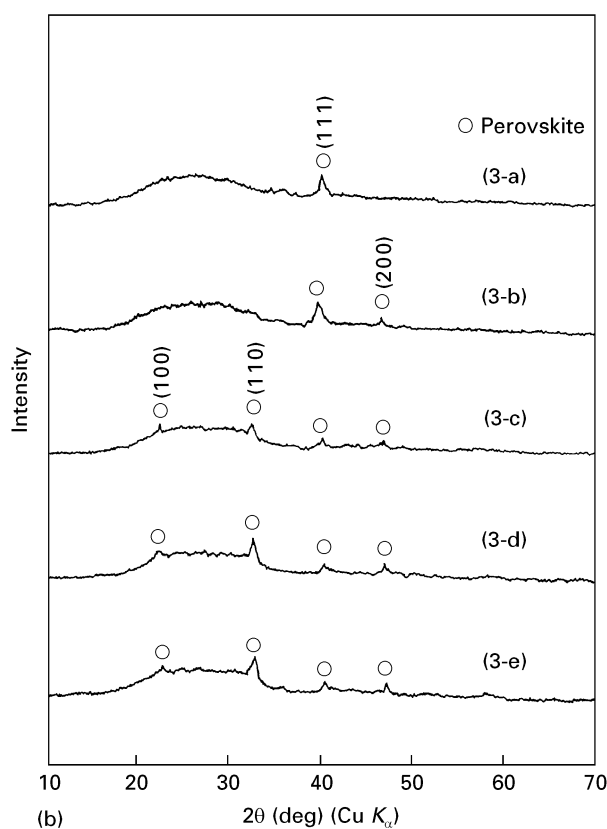
Fig. 6 shows the SEM pictures of the surface of the thin film samples prepared on ITO substrates by



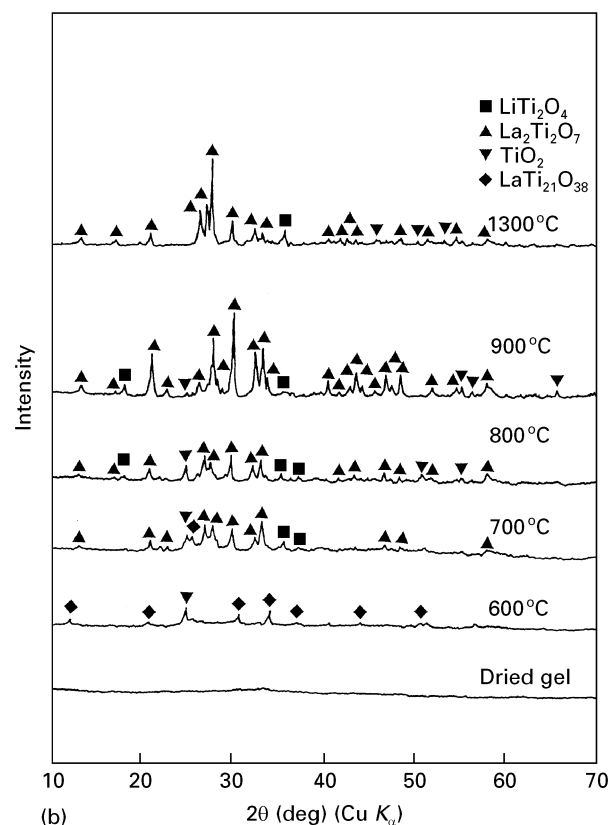
(a) 2θ (deg) ($\text{Cu } K_{\alpha}$)



(a) 2θ (deg) ($\text{Cu } K_{\alpha}$)



(b) 2θ (deg) ($\text{Cu } K_{\alpha}$)



(b) 2θ (deg) ($\text{Cu } K_{\alpha}$)

Figure 4 XRD patterns of $\text{La}_{0.5}\text{Li}_{0.5-x}\text{Pb}_{0.05+x/2}\text{TiO}_3$ ($x=0-0.4$) films prepared on (a) ITO and (b) NA substrates from series 3 solutions. Dip-coating and heat treatment at 700°C were repeated five times. The film thickness was about $0.2\ \mu\text{m}$.

Figure 5 XRD patterns of dried gel-derived products heat-treated at various temperatures. Solutions (a) 1-b and (b) 2-b were gelled and dried at 200°C for 2 h. Then the dried gels were heated at $600-1300^\circ\text{C}$ for 2 h.

repeating dip-coating and heat treatment at 700°C , 20 times. Roughness on a submicrometre scale and particles of about $0.04\ \mu\text{m}$ diameter were observed for the sample prepared from solution 1-b. A smooth

surface and particles of about $0.1\ \mu\text{m}$ diameter were observed for the sample from solution 2-b, whereas a very smooth surface with ultrafine particles was observed for the sample from solution 3-c.

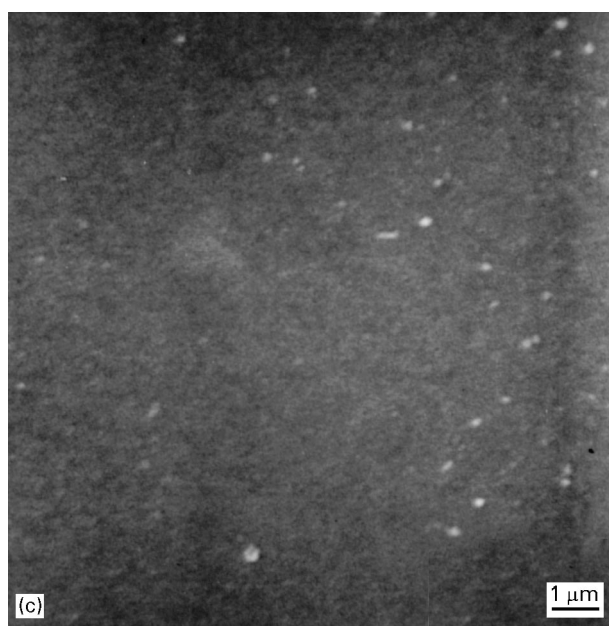
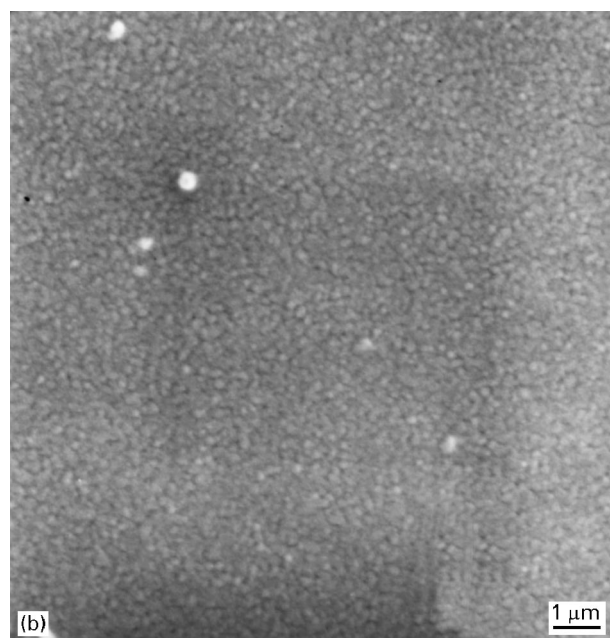
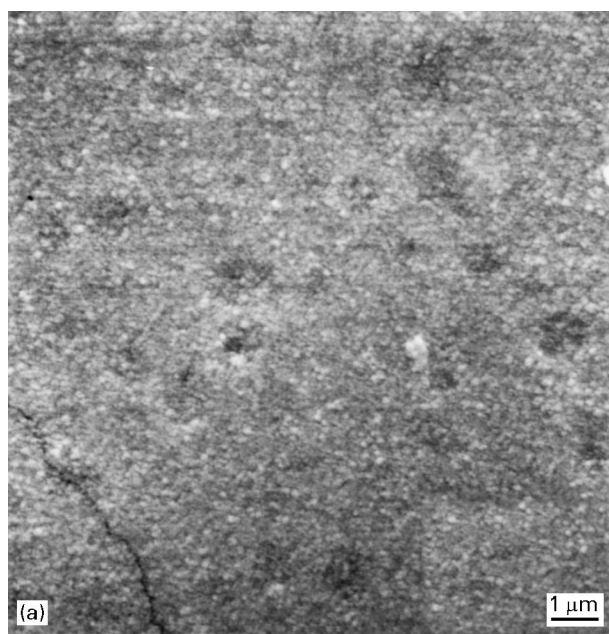


Figure 6 Scanning electron micrographs of $\text{La}_{0.5}\text{Li}_{0.5}\text{TiO}_3$ and $\text{La}_{0.5}\text{Li}_{0.3}\text{Pb}_{0.15}\text{TiO}_3$ films prepared on ITO substrates from solutions (a) 1-b, (b) 2-b, and (c) 3-c. Dip-coating and heat treatment at 700°C were repeated 20 times.

2-b suggests a higher porosity in the former sample. The higher refractive index of the sample from solution 3-c is due to the introduction of highly polarizable lead ions.

3.5. Electrical conductivity

Fig. 7 shows the in-plane a.c. electrical conductivity of the thin film samples. The conductivity at 120°C was about 10^{-8} – $10^{-7} \text{ S cm}^{-1}$, which is much smaller than the value reported for the sintered LLT materials ($4 \times 10^{-2} \text{ S cm}^{-1}$) [8]. The activation energy for conduction as shown in the figure was found to be larger than the value reported for the sintered LLT materials (0.15 eV) [8]. The sample prepared from solution 2-b showed a smaller conductivity and a smaller activation energy than that from solution 1-b. The sample prepared from solution 3-c showed a slightly smaller conductivity than those from solutions 1-b.

TABLE V Crystallite sizes, refractive indices and thickness of the films prepared on ITO substrates from solutions 1-b, 2-b and 3-c. Dip-coating and heat-treatment at 700°C were repeated 20 times

Solution	Crystallite size (nm)	Refractive index	Thickness (μm)
1-b	13	1.87	0.8
2-b	17	2.07	1.0
3-c	13	2.15	0.8

3.4. Refractive index

Refractive indices are shown in Table V for the thin film samples deposited on ITO substrates. The refractive indices were 1.87, 2.07 and 2.15 for the samples prepared from solutions 1-b, 2-b and 3-c, respectively. The lower refractive index of the sample from 1-b than

4. Discussion

4.1. Effects of the solution composition and substrate material on the crystallization behaviour

When ITO substrate was employed, LLT thin films were formed without impurity precipitation from alkoxide-based, series 1 solutions, whereas LLT films containing LiTi_2O_4 and $\text{La}_2\text{Ti}_2\text{O}_7$ as impurity phases were formed from acetate-based, series 2 solutions. In the gel films prepared from series 2 solutions, La^{3+} and Li^+ cations are possibly bridged by acetate anions with less extended, weakly branched metalloxane bonds. In particular, it should be noted that

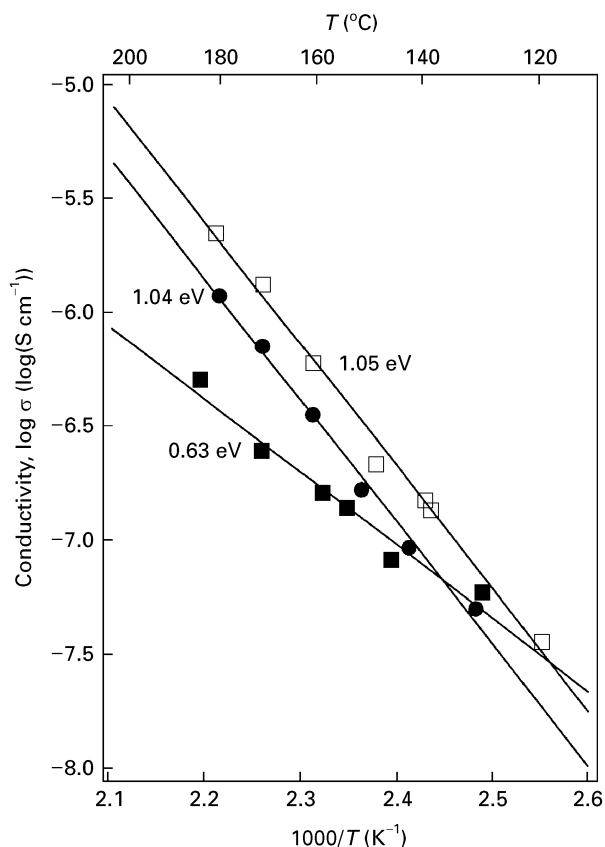


Figure 7 Arrhenius plots of a.c. electrical conductivity of the $\text{La}_{0.5}\text{Li}_{0.5}\text{TiO}_3$ films prepared on NA substrates from solutions (□) 1-b and (■) 2-b and of the film $\text{La}_{0.5}\text{Li}_{0.3}\text{Pb}_{0.15}\text{TiO}_3$ from solution (●) 3-c. Dip-coating and heat treatment at 700°C were repeated 20 times.

$\text{Li}(\text{CH}_3\text{COO})_2 \cdot 2\text{H}_2\text{O}$ is known to melt at a temperature as low as 70°C and to decompose at higher temperatures, and $\text{La}(\text{CH}_3\text{COO})_3 \cdot 1.5\text{H}_2\text{O}$ to release $0.5\text{H}_2\text{O}$ at 100°C and decompose at 120°C . This would result in inhomogeneous distribution of metal cations during the drying and pyrolysing processes due to the melting and decomposition of lithium and lanthanum acetate complexes. This explanation is supported by the fact that only undesired phases were precipitated without LLT formation in dried gel pieces from series 2 solutions, while LLT was formed without precipitation of impurity phases in dried gel pieces from series 1 solutions. Furthermore, the low melting and high volatility of lithium acetate complexes would cause the lower lithium content in the film from 2-b solution, and higher lithium deficiency would destabilize the LLT crystal structure, leading to the precipitation of the impurity phases.

Another factor affecting the precipitation of impurity phases is the substrate material. Even from series 2 solutions, impurity phases were not precipitated in the films when NA substrate was employed, although only LLT (1 1 1/2) diffraction peak was detected. This indicates that reaction products formed at the film/substrate interface provided heterogeneous nucleation sites and induced the precipitation of impurity phases. In the case of series 1 solutions, the films remained amorphous when NA substrate was employed. Well-extended, three-dimensional

metalloxane bonds in the gel are thought to stabilize the amorphous network structure.

In the series 2 solution-derived film samples deposited on ITO substrate, addition of acetylacetone to the solution suppressed the precipitation of $\text{La}_2\text{Ti}_2\text{O}_7$ impurity phases, and the increased H_2O content resulted in a slight increase in $\text{La}_2\text{Ti}_2\text{O}_7$ phase. Although the effect of acetylacetone is not very clear, its chelation of metal cations probably changed the coordination state and thermal stability of the metal complexes, resulting in suppression of the formation of impurity phases.

The partial substitution of lead for lithium suppressed the precipitation of impurity phases, which was observed in series 3-derived film samples deposited on ITO substrate. This is thought to result from the tolerance factor approaching unity by the element substitution, making the perovskite structure more stable.

4.2. The effects of the solution composition and substrate material on the crystal orientation

In the thin film samples prepared from series 2 solutions, preferred orientation of LLT (1 1 1/2) plane was observed when NA substrate was employed, whereas it was not observed when ITO substrate was employed. The partial substitution of lead for lithium depressed the preferred orientation. The preferred orientation observed here is not a result of epitaxial growth, because it occurred on glass surfaces. The ITO substrate has higher basicity than NA substrate (non-alkali aluminoborosilicate glass); the increase in the basicity of the substrate would cause the preferential adsorption of solution species with higher acidity. The acidity of the solutions, is increased by the substitution of lead for lithium. If we regard the deposition process as an acid–base reaction, change in the basicity (or acidity) of the substrate and solution influences the relative amount of chemical species that are preferentially adsorbed on the substrate, leading to change in the composition of the first molecular layer and affecting the orientation of the precipitated crystals.

4.3. Effects of the solution composition on the microstructure of the thin films

The scanning electron micrographs and refractive index data reveal that the LLT film sample derived from solution 1-b is more porous than that from solution 2-b. The reason for the evolution of the different microstructure is not clear. The difference in the structure and properties of the polymerized precursor species in sols, however, would influence the microstructure of the resultant films. Because the polymerized species formed in the alkoxide-based solution consist of well-extended, highly cross-linked metalloxane bonds, the resultant gel film has high resistance to compaction and shrinkage during drying [13], which would result in the formation of a porous film. On the contrary, because the polymerized species formed in

the acetate-based solution are built up with weak coordinative bonds between metal cations and acetate anions, the resultant gel film has low resistance against compaction and shrinkage during drying, resulting in a relatively dense film. The presence of the low-melting lithium acetate, which causes partial melting of the film, is another possible reason for the formation of the dense film.

4.4. Electrical conductivity

The present LLT film samples showed much lower electrical conductivities than the value reported for sintered LLT materials [8]. The low conductivity of the present films is basically thought to result from the high porosity, small crystallite size and a large amount of grain boundaries, all of which lower the lithium ion mobility. The film derived from acetate-based solution 2-b had a lower activation energy than that from alkoxide-based solution 1-b, which is thought to result from the larger crystallite or grain size and, possibly, higher crystallinity of the former film. Another possible reason for the lower activation energy of the solution 2-derived sample is thought to be due to a larger amount of lithium deficiencies. In other words, ionic conduction observed in the solution 2-derived sample can be regarded as "impurity conduction" and that in the solution 1-derived sample is "intrinsic conduction". The lower conductivity of the solution 2-derived sample may be due to the presence of impurity phases. The lead-containing sample showed lower conductivity than that from the solution 1-derived sample, probably because of the blocking of the lithium ion transport by the lead ions. D.c. electrical conductivities measured in the direction perpendicular to the film surface were more than three orders of magnitude lower than these a.c. conductivities, indicating that impurity phases of high electrical resistance are formed at the film/substrate interface.

5. Conclusions

Perovskite $\text{La}_{0.5}\text{Li}_{0.5}\text{TiO}_3$ (LLT) thin films, 0.2–1 μm thick, were prepared by the sol–gel method using the alkoxide-based solutions containing titanium alkoxide, lithium alkoxide and lanthanum alkoxide and the acetate-based solutions containing titanium alkoxide, lithium acetate and lanthanum acetate.

1. There was a tendency that impurity phases were more easily precipitated in the films derived from the acetate-based solutions than from the alkoxide-based solutions.

2. Addition of acetylacetone or partial substitution of lead for lithium in the acetate-based solutions, however, suppressed the impurity phase precipitation in the films.

3. Preferred orientation of the LLT (111/2) plane was observed in the films prepared from the acetate-based solutions when NA substrate was used, whereas the employment of the alkoxide-based solutions or ITO substrate and the partial substitution of lead for lithium reduced the preferred orientation.

4. Deficiency in lithium cations could be attained by the present route. The electrical conductivity of the films, however, was much lower than the value reported for the sintered materials.

Acknowledgement

The authors thank Mr Fumihiro Uratani, Osaka Prefectural Industrial Technology Research Institute, for ICP measurement and atomic absorption analysis.

References

1. G. ADACHI and H. AONO, *Ceramics* **27** (1992) 117 (in Japanese).
2. U. V. ALPEN, A. RABENAU and G. H. TALAT, *Appl. Phys. Lett.* **30** (1977) 621.
3. R. MERCIER, J.-P. MALUGANI, B. FAHYS and G. ROBERT, *Solid State Ionics* **5** (1981) 663.
4. H. WADA, M. MENETRIER, A. LEVASSEUR and P. HAGENMULLER, *Mater. Res. Bull.* **18** (1983) 189.
5. R. KANNO, Y. TAKEDA, K. TAKADA and O. YAMAMOTO, *J. Electrochem. Soc.* **131** (1984) 469.
6. J. KUWANO and A. R. WEST, *Mater. Res. Bull.* **15** (1980) 1661.
7. H. AONO, E. SUGIMOTO, Y. SADAOKA, N. IMANAKA and G. ADACHI, *J. Electrochem. Soc.* **137** (1990) 1023.
8. Y. INAGUMA, C. LIQUAN, M. ITOH and T. NAKAMURA, *Solid State Commun.* **86** (1993) 689.
9. J. BROUS, I. FANKUCHEN and E. BANKS, *Acta Crystallogr.* **6** (1953) 67.
10. P. V. PATIL and V. S. CHINCHOLKAR, *Curr. Sci.* **15** (1970) 348.
11. A. M. VARAPRASAD, A. L. SHASHI MOHAN, D. K. CHAKRABARTY and A. B. BISWAS, *J. Phys. C Solid State Phys.* **12** (1979) 465.
12. L. L. KOCHERGINA, N. B. KHAKHIN, N. V. POROTNIKOV and K. I. PETROV, *Russ. J. Inorg. Chem.* **29** (1984) 506.
13. C. J. BRINKER and G. W. SCHERER, "Sol–Gel Science: the Physics and Chemistry of Sol–Gel Processing" (Academic Press, New York, 1990) Ch. 13.

Received 19 January
and accepted 17 September 1996